11th ANKARA INTERNATIONAL AEROSPACE CONFERENCE **AIAC-2021-150**
8-10 September 2021 - METU, Ankara TURKEY

A HELICOPTER ROTOR MODELING AND MESHING SYSTEM

Halit Eldem Uzun* and Kaan Yutük†
METU & Turkish Aerospace
Ankara, Turkey

Seyyed Alialnaghi Madayen Shishvan,‡
Özgür Uğraş Baran§
and Mehmet Haluk Aksel¶
METU
Ankara, Turkey

ABSTRACT

Helicopter rotors in flight constitute a fairly complex wing geometry and exhibit motion in several axes. As a result, rotor motion creates quite complex flow patterns, and unlike fixed wings, flow around each rotor blade interacts with each other. These complexities make the analysis of the rotor flow is a challenge for CFD solvers. The challenge starts with very high requirements on the quality of the computational mesh. A modern helicopter rotor involves a number of different airfoil sections, complex profile blending, twists and other complexities. Moreover, blade tip geometry can be selected from a wide variety of candidates. In this study, we present the results of our fully automatized rotor geometry and solution domain generation tool. With the new tool a rotor with a very high complexity with any number of blades can be generated, and a very high quality multi-block and conformal meshes are produced.

INTRODUCTION

The flow field generated by the rotating blades is exceptionally complex and difficult to model and analyze. One of the most critical flow characteristics needed to predict rotorcraft performance is the accurate estimation of the rotor wake. In general, the rotor wake consists of a vortex sheet and a strong helical tip vortex. These vortices stay close to the rotor for many revolutions and induce a powerful three-dimensional velocity field, resulting in unsteady fluctuating airloads on the blades [Costes and et al., 2012]. Furthermore, helicopter rotor blade sections encounter a wide variety of Mach and Reynolds numbers from root to tip, ranging from subsonic to transonic, which may be detrimental to the stability and accuracy of the flow field simulations. There are also other aerodynamic issues, such as dynamic stall and shock-induced flow separation due to the local Mach number variation [Leishman, 2017]. These aerodynamic challenges require a very high-quality computational grid to obtain accurate CFD solutions with fast convergence.

*MSc. Student in Mechanical Engineering Department, Email: eldem.uzun@metu.edu.tr
†MSc. Student in Aerospace Engineering Department, Email: yutuk.kaan@metu.edu.tr
‡Phd. Student in Mechanical Engineering Department , Email: e248245@metu.edu.tr
§Assist. Prof. Dr. in Mechanical Engineering Department , Email: ubaran@metu.edu.tr
¶Prof. Dr. in Mechanical Engineering Department, Email: aksel@metu.edu.tr

The accuracy and convergence of any numerical flow field simulation are highly reliant on the quality of the grid used since stretched, skewed, and non-orthogonal cells may reduce the spatial discretization order, resulting in an increase in numerical dissipation. Mesh types can be classified into two categories based on their data structure and connectivity information, structured and unstructured grids differ in the mesh quality and solver requirements. Structured meshes can be aligned in the flow direction leading to more accurate results and a quick convergence behavior in CFD analyses than unstructured types; however, creating a single structured block grid that correctly discretizes the physical domain may not be possible for complex geometries. The multiblock structured grid method has been developed as an alternative approach to address the problems related to complex geometries. In order to meet the desired grid point distributions in complex regions composed of several sub-components, the physical domain is divided into a series of conformally-connected structured blocks. The multiblock technique can be extremely time-consuming since the grid dimensions and point distributions need to be specified for each block. This bottleneck can be overcome with a template-based mesh generation approach, and a parametric geometry definition would support the automation of grid templates.

There are different modelling tools in-service. Vehicle Sketch Pad (VSP) is the most widely used publicly accessible parametric geometry modeling application with a graphical user interface, developed by NASA for the conceptual design phase [Hahn , 2010] and based on the Rapid Airplane Modeler (RAM) [Gloudemans and et al., 1996]. TiGL is also an open-source geometry modeling library developed by the German Aerospace Research Centre (DLR) to ease the conceptual and preliminary aircraft and helicopter design workflows [Siggel and et al., 2019]. Another noteworthy open-source study is conducted by De Marco et al. [De Marco and et al., 2020]. They have developed a high-fidelity parametric geometry templates of external aircraft shapes. Vandenbrande et al. [Vandenbrande and et al., 2006] use the Boeing General Geometry Generator (GGG) as a parametric geometry modeler to automatize their design space exploration model. Rodriguez and Sturdza developed a geometry engine for preliminary aircraft design in the Java programming language, Rapid Geometry Engine (RAGE), which utilizes parametric geometry generation [Rodriguez & Sturdza, 2006].

There are also several studies of automatic multiblock grids utilizing the template-based approach. PADRAM is a design system that could create multiblock meshes for a set of problems and then be reused for a variety of similar geometries [Shahpar & Lapworth, 2003]. Zhang and Barakos [Zhang, T., & Barakos, G. N. , 2020] present a tool chain for compound rotorcraft, includes an automatic multiblock grid generation via ICEM CFD [Ansys Inc., 2021]. Köseömür and Baran describe an automated design code for missiles utilizing a multiblock structured grid generation method that relies on the geometry parameters provided by Missile DATCOM software [Köseömür, O. Z., & Baran, Ö. U. , 2019]. Allen developed an automatic multiblock structured grid generation scheme based on a modified transfinite interpolation [Allen, C. B., 2008]. Surface patches and a target number of grid cells for the entire domain are sufficient inputs for the scheme. Martinez et al. [Martinez et. al., 2015] developed a tool automating aerodynamic analysis stages of the flowfield around wind turbine rotor blades, named Aero-T, utilizing a set of python and shell scripts to drive IGG [IGG Numeca, 2021] to generate structured blocks.

The helicopter main rotor plays a significant role in vertical flight capability, moving in any direction and controlling the aircraft. Therefore, many analyses at various flight regimes and collective pitch angles must be performed throughout the design process of a helicopter rotor to achieve the desired requirements. A few days of setting up a new geometry model interactively and a couple of hours using a mesh generator to create an appropriate computational grid has been considered reasonable in the detailed design phase. Today, however, spending too much time on modeling and mesh generation is not acceptable in the conceptual and preliminary design stages. Many studies are conducted to accelerate the design stages of various aircraft and their components. However, only a few combine the parametric geometry modeler and grid generator in the same platform. Fewer studies focus on helicopter rotors. Motivating by these points, a fully automatic rotor geometry and

solution domain generation system is developed using multiblock structured grids. The parametric description of the rotor geometry involves several design variables. The mesh generator is automated using the geometry attributes provided by the modeler and satisfies the high-quality grid requirements for complex flow patterns around a helicopter rotor blade. The devised system is validated by well-known experimental results of the Caradonna-Tung rotor model.

METHOD

Rotor Definition System

The rotor modeling system is defined by all parameters needed to obtain its dimensional tree view. First, main inputs, including rotor radius and the number of blades, are given by the user. Then, the rotor blade is divided into the specified number of panels. Next, control cross-sections are placed side-by-side with equal distance for each panel. At least two cross-sections must be provided for a panel. Parameters such as taper ratio, sweep angle, dihedral angle, and twist can be distributed linearly or non-linearly for each panel. The camber line of the cross-sections is calculated automatically within the code, and blended profiles are achieved through the given blade thickness distributions.

In order to represent kink sections and other discontinuities accurately, panels are built piecewisely. However, the continuity condition between two subsequent panels can be changed. For example, a C^2 continuity can be imposed between two panels using a B-Spline interpolation. This feature is demonstrated in Figure 1.

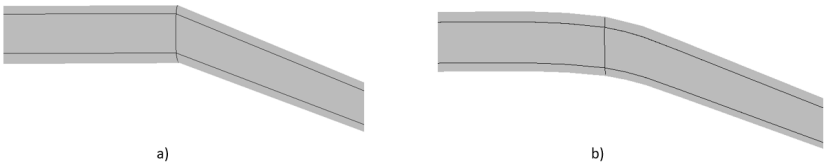

Figure 1: a) C^0 continuity, b) C^2 continuity

A rotor blade comprises six panels with an anhedral, tapered, and swept wing is shown in Figure 2 as an example. The planform and sides view of the blade tip is also demonstrated.

Geometry Processing

Control cross-sections are built employing NURBS curves, then stacks of airfoils are lofted spanwise to generate rotor blades. Surface skinning can be performed linearly, or a B-spline of 3rd degree can be used. The B-spline and NURBS curve modeling algorithms applied in the developed system are derived from formulations in the standard textbooks [Piegl and Tiller, 1995].

B-Spline Curves:

Let $T = \{t_0, ..., t_m\}$ be a increasing sequence of real numbers, such that $t_i < t_{i+1}$ for $i = 0, ..., m$. T is the knot vector, and t_i numbers are named as knots. Then the ith B-Spline basis function of pth degree, indicated as $N_{i,p(t)}$, is defined by

$$N_{i,0}(t) = \begin{cases} 1 & if\ u_i \leq u \leq u_{i+1} \\ 0 & otherwise \end{cases}$$

$$N_{i,p}(t) = \frac{t - t_i}{t_{i+p} - t_i} N_{i,p-1}(t) + \frac{t_{i+p+1-t}}{t_{i+p+1-t} - t_{i+1}} N_{i+1,p-1}(t) \tag{1}$$

A pth degree B-Spline curve is defined by

$$C(t) = \sum_{n}^{i=0} N_{i,p}(t)\mathbf{P}_i \qquad a \leq t \leq b \tag{2}$$

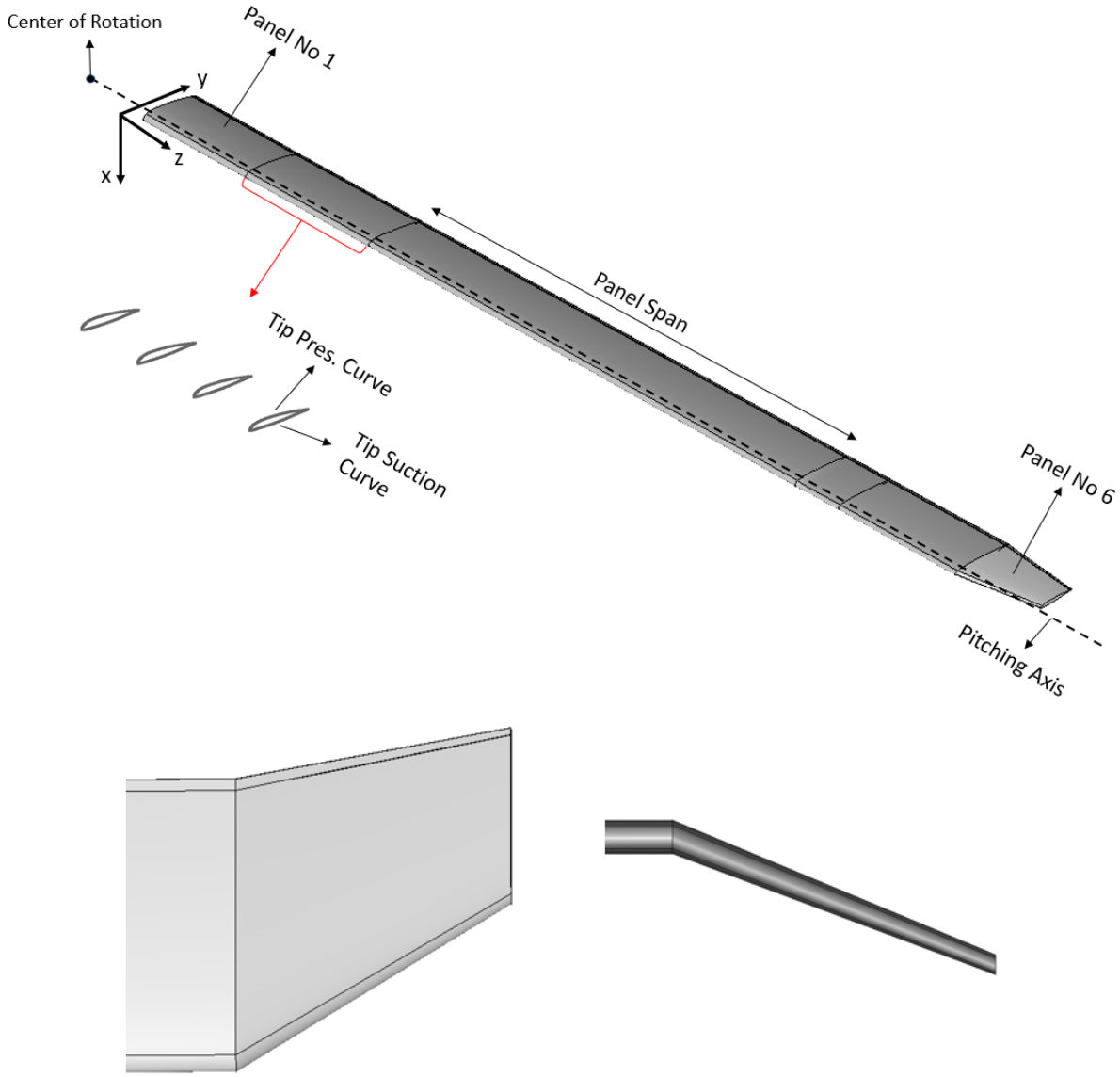

Figure 2: Isometric View of the Generated Model

NURBS Curves:

A pth degree NURBS curve is efined by

$$C(t) = \frac{\sum_{i=0}^{n} N_{i,p}(t)\omega_i \mathbf{P}_i}{\sum_{i=0}^{n} N_{i,p}(t)\omega_i} \tag{3}$$

Defining a rational basis functions, $R_{i,p}(t)$:

$$R_{i,p} = \frac{N_{i,p}(t)\omega_i}{\sum_{j=0}^{n} N_{j,p}(t)\omega_j}$$

Then, Eq. (3) becomes

$$C(t) = \sum_{i=0}^{n} N_{i,p}(t) R_{i,p} \mathbf{P}_i \tag{4}$$

A $3rd$ degree NURBS definition is directly used as fitting curves without further interpolation or approximation for computational simplicity and fast solutions.

Mesh Topology

For spatial discretization, algebraic multiblock structured grid generation methods have been used. Although structured grids are extremely labor-intensive, an automatized mesh template is produced for any rotor model created by given parameters. O-type grid topology is applied around the rotor blade in the chordwise direction, and H-type topology is used in the spanwise direction. Then, H-type blocks are assigned to fill the computational domain up to far-field. Each block is composed of hexahedral elements. The first-cell height, cell number for boundary layer and the growth rate are given to the code as inputs. The collective pitch and precone angles can also be modified to investigate the hover performance.

The six-boundary transfinite interpolation method is employed in multi-block structured grid generation. The Boolean sum of three projectors can be used to formulate the interpolation as:

$$\begin{aligned}\overrightarrow{r}(u,v,w) &= P_u \cdot P_v \cdot P_w \\ &= P_u + P_v + P_w - P_uP_v - P_uP_w - P_vP_w + P_uP_vP_w \end{aligned} \tag{5}$$

where $\overrightarrow{r}$ denotes the transformation from computational to physical domain and u, v, and w expresses the directions in the normalized parametric coordinates. Three projectors which interpolate in u, v, w directions to match specified values of grid point coordinates, can be explained as follows,

$$\begin{aligned} P_u(\overrightarrow{r}) &= L_0(u)\overrightarrow{r}(0,v,w) + L_1(u)\overrightarrow{r}(1,v,w) \\ P_v(\overrightarrow{r}) &= L_0(v)\overrightarrow{r}(u,0,w) + L_1(v)\overrightarrow{r}(u,1,w) \\ P_w(\overrightarrow{r}) &= L_0(w)\overrightarrow{r}(u,v,0) + L_1(w)\overrightarrow{r}(u,v,1) \end{aligned} \tag{6}$$

where $\overrightarrow{r}(0,v,w)$, $\overrightarrow{r}(1,v,w)$, $\overrightarrow{r}(u,0,w)$, $\overrightarrow{r}(u,1,w)$, $\overrightarrow{r}(u,v,0)$,and $\overrightarrow{r}(u,v,1)$ describe six boundary of the 3D block domain. $L_0(s)$ and $L_1(s)$ are blending funtions for any curvilinear direction and can be defined as:

$$L_0 = 1 - s \quad \text{and} \quad L_1 = s \tag{7}$$

Various blending functions such as Lagrange, Hermite, B-spline, and NURBS can be combined in different directions.

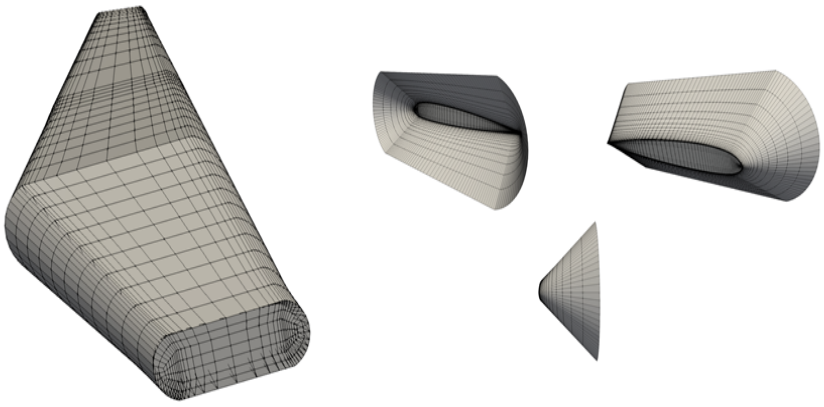

Figure 3: O-type grid around a blade

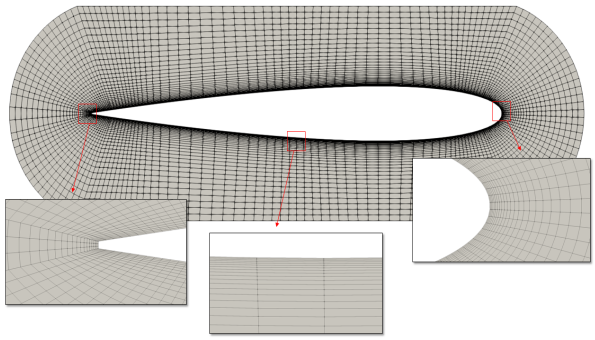

Figure 4: Boundary Layer Mesh Around an Airfoil Section

In the Figure 3, there can be seen isometric view of O-type grid around a blade with its conic extension at the blade tips. Figure 4 gives more detail views for the boundary layer mesh and how airfoil section of the blade is meshed.

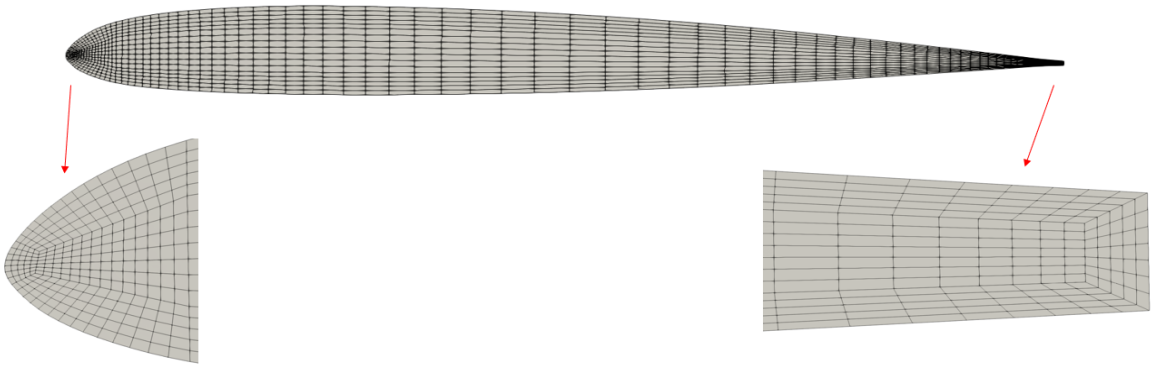

Figure 5: Blade Tip Mesh Structure

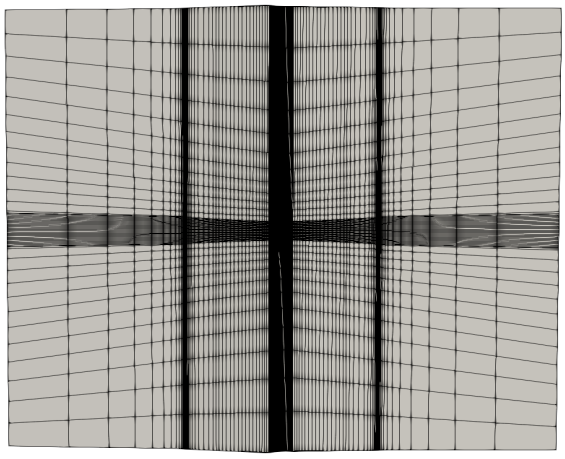

Figure 6: Plane view of the template

Tip section is the most important part of the rotor blade because it is the main source of the physical complexities. Therefore, this section demands highest quality meshes. Butterfly type meshing is preferred (Figure 5). Moreover, plane view of the automatized helicopter rotor mesh template can be seen in Figure 6 and the overview of the template is shown in Figure 7.

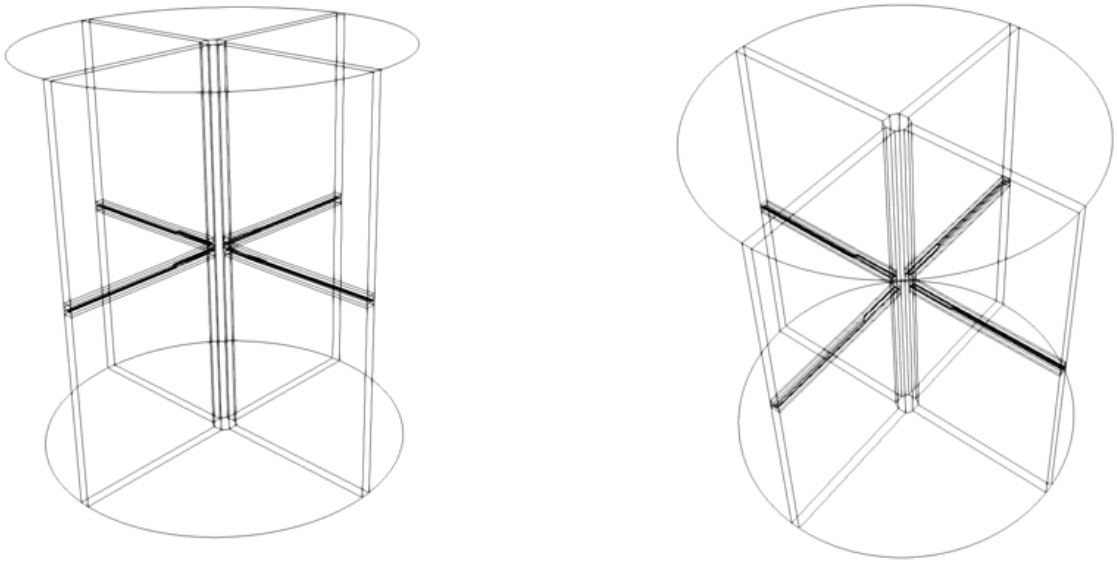

Figure 7: Automatized Mesh Template

RESULTS

In this study, Caradonna-Tung helicopter rotor blade is preferred for validation of the modelling and meshing tool kit. Flow field solutions are obtained by Stanford University Unstructured (SU^2) Code [Economon and et al., 2017].

Mesh Metrics	
Mesh	Number of Nodes
Course Mesh	800K
Middle Mesh	1.4M
Fine Mesh	2.3M

Table 1: Mesh Sizes Used in Mesh Independency Study

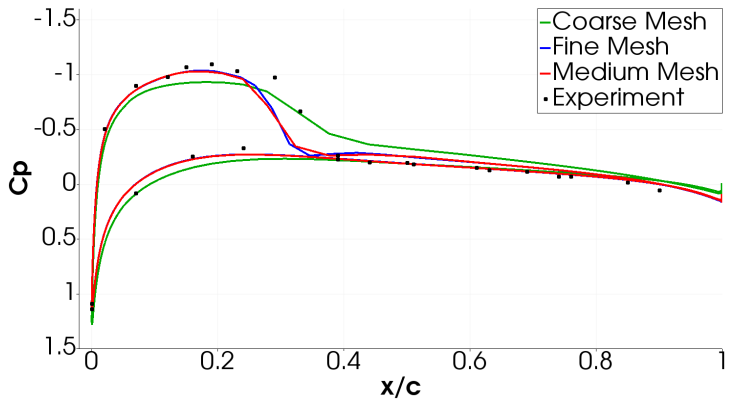

Figure 8: O-type grid around a blade

Test Case 1

The first test case is a transonic flow where the collective pitch angle is 8 degrees, and the tip Mach number is 0.877. Figure 8 indicates pressure distributions at $r/R = 0.96$ for different mesh sizes.

There is no important difference between the solutions obtained on medium and fine grids. Pressure distributions for this test case are given in Figure 9. The flow is entirely subsonic at $r/R = 0.6$, while a shock formation develops on the outer 20% of the blade, $r/R = 0.80$, 0.89, and 0.96.

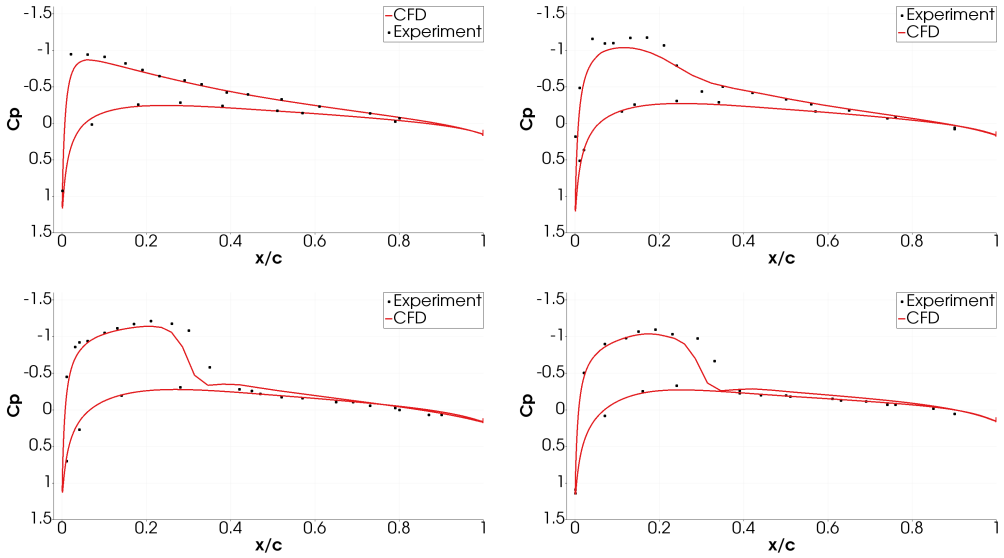

Figure 9: Comparison of Pressure Coefficient Distribution for Caradonna-Tung Geoemtry at $M_{tip} = 0.877$

Test Case 2

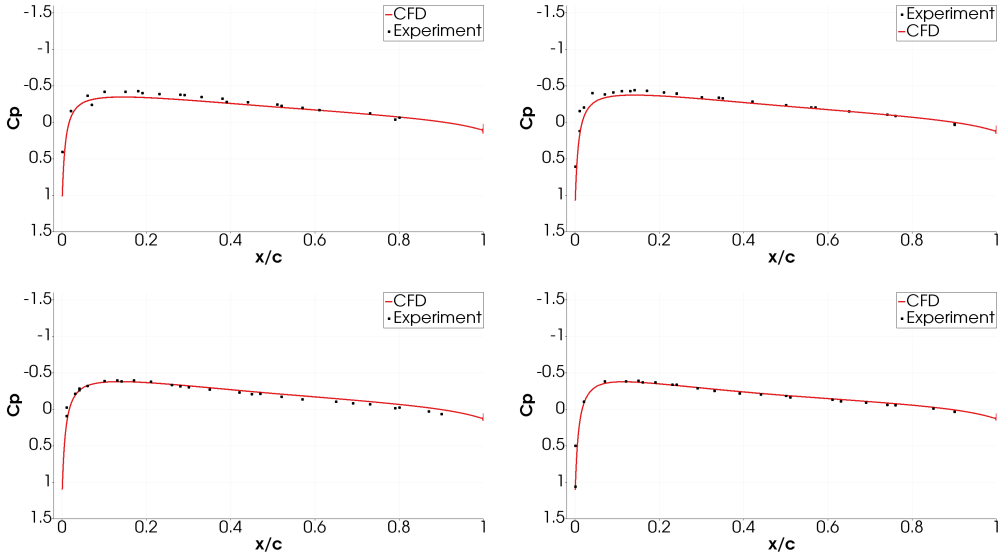

Figure 10: Comparison of Pressure Coefficient Distribution for Caradonna-Tung Geoemtry at $M_{tip} = 0.520$

The second test case is non-lifting at zero collective pitch angle with a tip Mach number of 0.52. Pressure coefficient distributions are shown in Fig. 10. In this case, the agreement between results from the viscous simulation and the experimental data for both the pressure and suction surface is satisfactory.

Test Case 3

The collective pitch angle is set to 8 degrees with a tip Mach number of 0.439 for the third test case. Pressure coefficient distributions are given in Fig. 11. The figures show a good agreement between the experimental and computed results for the pressure surface. Pressure distributions are slightly under-predicted at the leading edge of suction surfaces for all stations. The surface of constant vorticity in Fig. 12 shows a tip vortex that is produced at the tip of the blades and follows a helical shape.

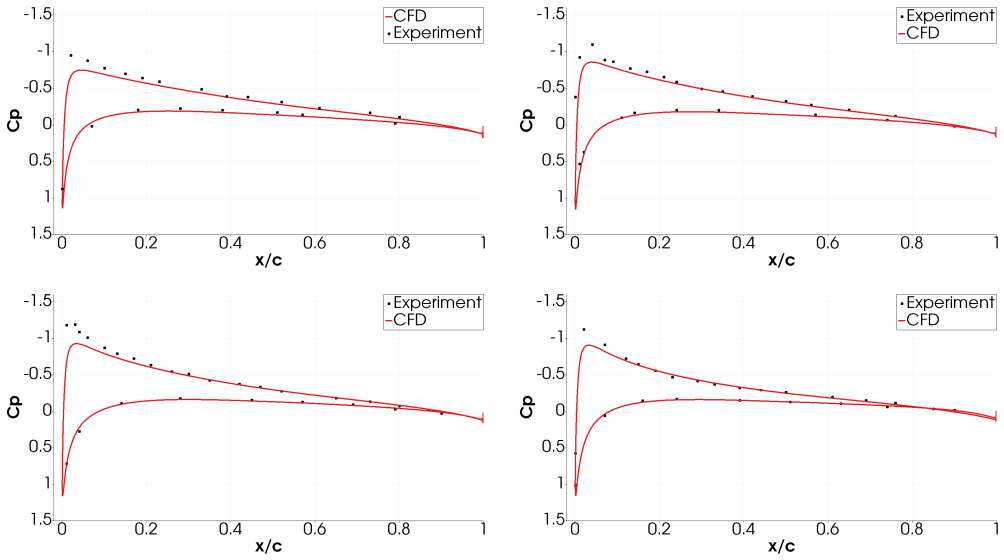

Figure 11: Comparison of Pressure Coefficient Distribution for Caradonna-Tung Geoemtry at $M_{tip} = 0.439$

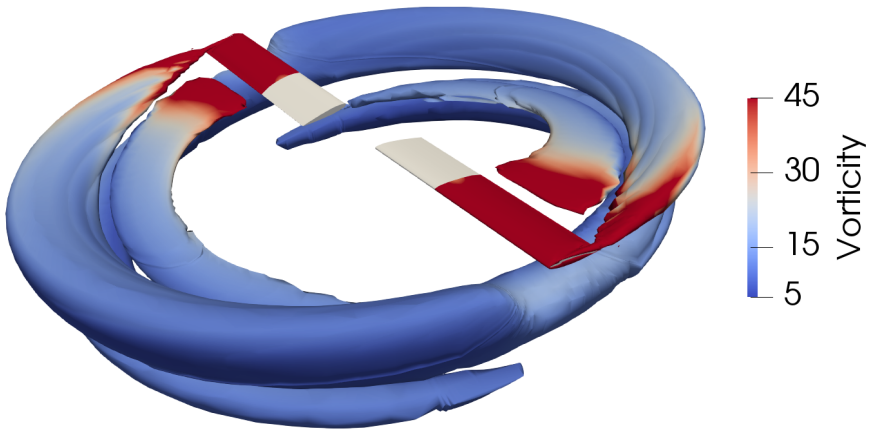

Figure 12: Isosurfaces of Q-Criteria colored with Vorticity for Caradonna Tung Rotor

CONCLUSIONS

In this study, an automatic and robust structured multiblock conformal mesh generation with parametric geometry attribute is developed to be included in the conceptual and preliminary design phases of a helicopter. The parametric geometry modeler within the system requires a set of design parameters. Complex rotor geometries with any number of blades can be generated through linear or non-linear distribution of specified parameters. The six-boundary transfinite interpolation method is employed to achieve multiblock conformal mesh generation. A set of inputs, including collective pitch, precone angle, grid dimensions, and boundary layer parameters, can be modified by the user. Viscous flow solutions are validated by comparing with the experimental results of the Caradonna-Tung rotor.

References

Allen, C. B. (2008) *Towards automatic structured multiblock mesh generation using improved transfinite interpolation*, International Journal for Numerical Methods in Engineering, Vol 74(5), p: 697-733, 2008.

Ansys Inc (2021) *ANSYS Meshing*. Automatic Multiblock Structured Grids, Last accessed: 2021-08-03, 2021.

Costes, M., Renaud, T., & Rodriguez, B. (2012) *Rotorcraft simulations: a challenge for CFD*, International Journal of Computational Fluid Dynamics, Vol 26, p: 383-405, 2012. doi:10.1080/10618562.2012.726710.

De Marco, A., Di Stasio, M., Della Vecchia, P., Trifari, V., and Nicolosi, F. (2020) *Automatic modeling of aircraft external geometries for preliminary design workflows*, Aerospace Science and Technology, Vol 98, p: 105667, 2020. doi:10.1016/j.ast.2019.105667.

Economon, T. D., Alonso, J. J., Albring, T. A., & Gauger, N. R. (2017) *Adjoint formulation investigations of benchmark aerodynamic design cases IN SU2*, 35th AIAA Applied Aerodynamics Conference, 2017. doi:10.2514/6.2017-4363

Gloudemans, J., Davis, P., & Gelhausen, P. (1996, January) *A rapid geometry modeler for conceptual aircraft*, In 34th aerospace sciences meeting and exhibit, p: 52, 1996.

Hahn, A. (2010, Jan) *Vehicle sketch pad: a parametric geometry modeler for conceptual aircraft design*, 48th AIAA Aerospace Sciences Meeting Including the New Horizons Forum and Aerospace Exposition, p: 657, Jan 2010.

IGG Numeca (2021) *IGG Numeca Meshing*, IGG Numeca Meshing, Automatic Multiblock Structured Grids, 2021.

Köseömür, O. Z., & Baran, Ö. U. (2019) *Automatic Mesh Generator Integrated Missile Design Tool Development*, 2019.

Leishman, J. G. (2017) *Principles of helicopter aerodynamics*, Cambridge, United Kingdom: Cambridge University Press, 2017.

Martinez, J. A. V. I. E. R., Doerffer, P., Szulc, O., & Tejero, F. (2015) *Aerodynamic analysis of wind turbine rotor blades*, Task Q, Vol 19(2), p: 129-140, 2015.

Piegl, L. A., and Tiller, W. (1995) *The NURBS book*, Berlin: Springer, 1995.

Rodriguez, D., & Sturdza, P. (2006, Jan) *A rapid geometry engine for preliminary aircraft design*, 44th AIAA Aerospace Sciences Meeting and Exhibit, p: 929, Jan 2006.

Seddon, J. M., and Newman, S. (2011) *Basic Helicopter Aerodynamics*, Hoboken: Wiley, 2011.

Shahpar, S., & Lapworth, L. (2003, Jan) *PADRAM: Parametric design and rapid meshing system for turbomachinery optimisation*, In Turbo Expo: Power for Land, Sea, and Air, Vol 36894, p: 579-590, Jan 2003.

Siggel, M., Kleinert, J., Stollenwerk, T., & Maierl, R. (2019) *TiGL: an open source computational geometry library for parametric aircraft design*, Mathematics in Computer Science, Vol 13(3), p: 367-389, 2019.

Vandenbrande, J., Grandine, T., & Hogan, T. (2006, Jan) *The search for the perfect body: Shape control for multidisciplinary design optimization*, In 44th AIAA Aerospace Sciences Meeting and Exhibit, p: 928, Jan 2006.

Zhang, T., & Barakos, G. N. (2020) *Development of Simulation Tools for High Fidelity Analysis of Compound Rotorcraft*, AIAA Scitech 2020 Forum, p: 1258, 2020.